Published in final edited form as:
Mol Cell Biochem. 2009 February ; 322(1-2): 53–62. doi:10.1007/s11010-008-9939-6.

Inhibition of matrix metalloproteinases improves left ventricular function in mice lacking osteopontin after myocardial infarction

Prasanna Krishnamurthy[1], **J. Thomas Peterson**[2], **Venkateswaran Subramanian**[1], **Mahipal Singh**[1], and **Krishna Singh**[1,*]

[1]Department of Physiology, James H Quillen College of Medicine, James H Quillen Veterans Affairs Medical Center, East Tennessee State University, Johnson City, TN 37614

[2]Cardiovascular Biology, Pfizer Global Research and Development, 2800 Plymouth Road, Ann Arbor, MI 48105

Abstract

Osteopontin (OPN) plays an important role in left ventricular (LV) remodeling after myocardial infarction (MI) by promoting collagen synthesis and accumulation. This study tested the hypothesis that MMP inhibition modulates post-MI LV remodeling in mice lacking OPN. Wild-type (WT) and OPN knockout (KO) mice were treated daily with MMP inhibitor (PD166793, 30 mg/kg/day) starting 3 days post-MI. LV functional and structural remodeling was measured 14 days post-MI. Infarct size was similar in WT and KO groups with or without MMP inhibition. M-mode echocardiography showed greater increase in LV end-diastolic (LVEDD) and end-systolic diameters (LVESD) and decrease in percent fractional shortening (%FS) and ejection fraction in KO-MI versus WT-MI. MMP inhibition decreased LVEDD and LVESD, and increased %FS in both groups. Interestingly, the effect was more pronounced in KO-MI group versus WT-MI ($P<0.01$). MMP inhibition significantly decreased post-MI LV dilation in KO-MI group as measured by Langendorff-perfusion analysis. MMP inhibition improved LV developed pressures in both MI groups. However, the improvement was significantly higher in KO-MI group versus WT-MI ($P<0.05$). MMP inhibition increased heart weight to body weight ratio, myocyte cross sectional area, fibrosis and septal wall thickness only in KO-MI. Percent apoptotic myocytes in the non-infarct area was not different between the treatment groups. Expression and activity of MMP-2 and MMP-9 in the non-infarct area was higher in KO-MI group 3 days post-MI. MMP inhibition reduced MMP-2 activity in KO-MI with no effect on the expression of TIMP-2 and TIMP-4 14 days post-MI. Thus, activation of MMPs contributes to reduced fibrosis and LV dysfunction in mice lacking OPN.

Keywords

Osteopontin; MMPs; Extracellular matrix; apoptosis; heart failure

Introduction

Osteopontin (OPN), also called cytokine Eta-1, contains Arg-Gly-Asp-Ser cell-binding sequence and interacts with αvβ1, αvβ3, and αvβ5 integrins and CD44 receptors (1). Heart expresses OPN at low levels under basal conditions (2,3). However, expression of OPN increases markedly under several pathophysiological states (2–5). Using OPN knockout (OPN

*__Correspondence__: Krishna Singh, Ph.D., Dept of Physiology, James H Quillen College of Medicine, East Tennessee State University, PO Box 70576, Johnson City, TN 37614, Ph: 423-439-2049, Fax: 423-439-2052, E-mail: E-mail: singhk@etsu.edu .

Conflict of Interest/Disclosure: None

KO) mice and myocardial infarction (MI) as a model of myocardial remodeling, our laboratory demonstrated that increased OPN expression plays an important role in regulating post-MI LV remodeling by promoting collagen synthesis and accumulation (2).

The extracellular matrix (ECM) of the heart is considered to play an important role in LV remodeling. Homeostasis of ECM (degradation and accumulation) is controlled by zinc-dependent interstitial enzymes, matrix metalloproteinases (MMPs) and their tissue inhibitors (TIMPs) (6–9). Of these, expression of MMP-2 is of particular interest because MMP-2 degrades ECM substrates including Type IV collagen, laminin, elastin, and interstitial fibrillar collagen (10,11). Cardiac specific expression of MMP-2 induces development of cardiac contractile dysfunction in the absence of superimposed injury (12). Targeted deletion of MMP-2 attenuates early rupture and improves percent fractional shortening (%FS) in mice post MI (13). MMP-2 is also shown to be associated with increased cardiac myocyte apoptosis following β-AR stimulation (14).

OPN is suggested to modulate the activity of matrix metalloproteinases (MMPs) in various cell types (15–17). OPN mediates effects of cell-matrix and cell-cell interactions by interacting with several integrins (18–20). Previously, we have provided evidence that OPN inhibits interleukin-1β-stimulated increases in the expression and activity of MMP-2 and −9 in isolated adult rat cardiac fibroblasts (17). Here we tested the hypothesis that MMP inhibition influences post-MI LV remodeling in mice lacking OPN.

Materials and Methods

Vertebrate Animals

All experiments were performed in accordance with the protocols approved by the Institutional Animal Care and Use Committee. Mice lacking OPN (KO mice) and wild-type mice (WT mice) were of a 129X black Swiss hybrid background (21). Genotyping was carried out by polymerase chain reaction analysis using the primers suggested by Liaw et al (21).

Myocardial infarction and MMPs inhibition

Age-matched mice (~4 months) were subjected to MI by ligation of left anterior descending (LAD) artery as described previously (22). The sham-operated animals underwent the same procedure except the LAD ligation. MMPs inhibition was achieved by daily oral gavage of PD 166793 (PD; 30 mg/kg body weight/day) starting 3 days post-MI until 14 days post-MI. PD is a selective MMP inhibitor and does not inhibit other metalloproteases like tumor necrosis factor-α (23). The dose of PD and time of treatment are chosen based on previously published report in mice (24).

Echocardiographic studies

In vivo heart function and chamber dimensions were assessed using a Toshiba Aplio 80 Imaging System (Tochigi, Japan) equipped with a 12-MHz transducer (PLT-1202S) as described (25). M-mode tracings were used to measure LV wall thickness, and end-systolic (LVESD) and end-diastolic dimensions (LVEDD). Percent fractional shortening (%FS) and ejection fractions (EF) were calculated (26). Measurements were averaged from nine different readings per mouse.

Langendorff Preparation

Langendorff perfusion was carried out by the method described (2). The hearts were paced at 7 Hz. A small fluid-filled balloon was placed in the LV and connected to a pressure transducer for determination of LV pressures. Systolic and diastolic pressure-volume relationships were determined by increasing the LV balloon volume in 5-μL increments using an airtight Hamilton

syringe. The balloon volume was increased until peak LV developed pressure was reached and a further increase led to decrease in LV developed pressure.

Morphometric studies

After Langendorff studies, the intra-LV balloon was filled to a diastolic pressure of 5 mmHg, and the hearts were arrested in diastole with KCl (30 mmol/L) followed by perfusion fixation with 10% buffered formalin. Hearts were weighed and cut into 3 slices (apex, mid-LV and base) and paraffin embedded. The morphometric analyses, including myocyte cross-sectional area and fibrosis, were carried out on Masson's trichrome stained sections (4 μm) using Bioquant image analysis software (Nashville, TN). To measure myocyte cross-sectional area, suitable areas with nearly circular capillary profiles and myocyte nuclei were used.

TUNEL-staining

To detect apoptosis, terminal deoxynucleotidyl transferase-mediated dUTP nick end-labeling (TUNEL) staining was carried out on 4-μm-thick paraffin embedded sections as per manufacturer's instructions (cell death detection assay kit, Roche) as described (27). TUNEL-positive nuclei clearly seen within the cardiac myocytes were counted. The index of apoptosis was calculated as the percentage of apoptotic myocyte nuclei/total number of nuclei.

Western blot analysis

Lysates from LV tissues were prepared in ice-cold RIPA buffer as described (27). Proteins (75 μg) were electrophoresed and transferred onto PVDF membrane. The membranes were incubated with antibodies against MMP-2 or MMP-9 (Chemicon Inc.) and TIMP-2 (Santa Cruz Biotech), TIMP-4 (Chemicon Inc). The immune complexes were detected using chemiluminescence reagents (Pierce Biotech.). The membranes were stripped and probed with GAPDH antibodies to optimize protein loading in each lane. Band intensities were quantified using Kodak photodocumentation system (Eastman Kodak Co.). The data are expressed as fold change vs WT-sham.

In-gel zymography

MMP activity in LV tissue lysate containing 50 μg of protein was measured using gelatin in-gel zymography (17). Clear and digested regions representing MMPs activity were quantified using a Kodak documentation system, and molecular weights were estimated using prestained molecular weight markers.

Statistical analyses

Data are represented as mean ± SE. Data were analyzed using student *t* tests or one-way analysis of variance (ANOVA) and a post hoc Tukey's test. Probability (P) values of <0.05 were considered to be significant.

Results

Morphometric studies

There was no significant change in the body weights 14 days post-MI with or without MMP inhibition. Mortality rate was the same in the two groups with or without MMP inhibition. MI size, measured as a percentage of the LV circumference, was not different between WT-MI and KO-MI groups (Table 1). MMP inhibition had no effect on MI size. The heart weight to body weight (HW/BW) ratio was increased in both MI groups. However, the increase in HW/BW was significantly higher in WT-MI as compared to KO-MI group. MMP inhibition increased HW/BW ratio in KO-MI group ($P<0.05$; KO-MI+PD versus KO-MI, Table 1), not in WT-MI.

Echocardiographic parameters

M-mode echocardiography showed no difference in LVESD, LVEDD, septal wall thicknesses, %FS and EF (%) between the WT and KO groups at base line. MI increased LVEDD and LVESD in both MI groups. However, the increase in LVEDD and LVESD was significantly higher in KO-MI as compared to WT-MI and sham groups (P<0.001 versus KO-sham; P<0.05 versus WT-MI; Table 2). MMP inhibition decreased LVEDD and LVESD in both MI groups. The decrease in LVEDD and LVESD was significantly higher in KO-MI+PD group (P<0.01 versus KO-MI; Table 2). Percent FS and EF (%) were significantly decreased in both MI groups. However, the decrease in %FS and EF (%) was significantly higher in KO-MI group as compared to WT-MI. MMP inhibition attenuated MI-induced decreases in %FS and EF (%) in both MI groups. Interestingly, this attenuation in %FS and EF (%) was significantly higher in KO-MI+PD group. Septal wall thicknesses (diastolic and systolic) were increased in both MI groups. However, the increase in septal wall thicknesses was significantly lower in KO-MI group when compared to WT-MI. MMP inhibition increased septal wall thicknesses in only in KO-MI group.

LV Pressure-Volume Relationships

Langendorff perfusion analysis indicated no differences in the LV end-diastolic pressure (LVEDP) - and LV developed pressure (LVDP) - volume relationship between the two sham groups (Fig. 1). The LVEDP-volume curve exhibited a significant rightward shift in both MI groups. However, this rightward shift was greater in KO-MI group when compared to WT-MI, indicating greater LV dilation in KO-MI group. MMP inhibition decreased this rightward shift in the curve in the KO-MI group, not in WT-MI (P<0.05 vs WT-MI+PD; Fig 1A). The LVDP-volume relationship was significantly decreased in KO-MI group as compared to WT-MI and sham (P<0.05 vs KO-sham and WT-MI; Fig 1B). MMP inhibition significantly improved LVDP in both MI groups. However, this improvement was significantly higher in KO-MI+PD when compared to WT-MI+PD group (P<0.05 vs WT-MI+PD).

Myocyte cross-sectional area

Analysis of myocyte cross-sectional area using trichrome-stained sections indicated increased myocyte cross-sectional area in both MI groups. However, the increase in myocyte cross-sectional area which was significantly higher in WT-MI when compared to KO-MI (Fig 2). MMP inhibition increased myocyte cross sectional area only in KO-MI, not in WT-MI group.

Apoptosis and fibrosis

The number of TUNEL-positive myocytes in the non-infarct area was not significantly different between the two MI groups. MMP inhibition had no effect on the number of apoptotic myocytes in either groups (percent apoptosis; WT-sham, 0.33±0.03; WT-MI, 0.43±0.06; KO-sham, 0.32±0.09; KO-MI, 0.34±0.07; WT-MI+PD, 0.31±0.09; KO-MI+PD, 0.23±0.03; P=NS).

Quantitative analysis of trichrome-stained sections indicated increased fibrosis in WT-MI group as compared to KO-MI (p<0.005 vs KO-MI; Table 1). MMP inhibition significantly increased fibrosis only in KO-MI+PD, not in WT-MI+PD group (p<0.01 vs KO-MI; Table 1).

Expression and activity of MMPs in the heart post-MI

MMP (MMP-2 and-9) expression and activity increases rapidly in the heart post-MI (28,29). MMP-2 promoter activity in the heart increases within 24h post-MI, while MMP-9 promoter activity was increased in the heart 3 days post-MI (28). Here, we first examined MMP expression and activity in the infarct and non-infarct LV regions 3 days post-MI. Western blot analysis indicated increased MMP-2 protein levels to a similar extent in the infarct area of both

MI groups. However, increased MMP-2 protein levels were only observed in the non-infarct area in KO-MI group, not in WT-MI (Fig 3A). Likewise, MMP-9 protein levels were increased to a similar extent in the infarct area of both MI groups. However, increased MMP-9 protein levels were only observed in the non-infarct area in KO-MI group, not in WT-MI (Fig 3B). Analysis of MMP activity using gelatin in-gel zymography indicated increased MMP-2 and MMP-9 activity to a similar extent in both MI groups in the area of infarct (Fig 4A). In the area of non-infarct, significant increase in MMP-2 and MMP-9 activities was observed only in the KO-MI group (Fig 4B).

Analysis of MMP activity 14 days post MI indicated increased MMP-2 activity in the non infarct area in both MI groups. However, the increase in MMP-2 activity was significantly higher in the KO-MI group when compared to WT-MI ($P<0.05$ vs WT-MI; n=4; Figure 5). MMP inhibition significantly reduced MMP-2 activity in KO-MI group, not in WT-MI group ($P<0.01$ vs KO-MI; n=4; Fig 5). Gelatin in-gel zymography did not show a noticeable activity or change in MMP-9 activity 14 days post-MI with or without MMP inhibition in either group (data not shown).

Expression of TIMP-2 and TIMP-4 in the heart post-MI

Tissue inhibitors of MMPs (TIMPs) play an important role in regulation of MMPs activity (8,30). Therefore, we next measured expression of TIMPs in the heart post-MI. Western blot analysis indicated no change in TIMP-2 or TIMP-4 protein levels in the non-infarct area in WT or KO groups 14 days post-MI (fold change vs sham, TIMP-2, WT-MI, 1.19±0.04, KO-MI, 1.12±0.06, n=4; TIMP-4, WT-MI, 1.23±0.1; KO-MI, 1.14±0.1, n=4; Figure 6). MMP inhibition did not significantly change the levels of TIMP-2 and TIMP-4 in both MI groups.

Discussion

Expression of OPN increases in the heart during hypertrophy and failure (2,3,5). Mice lacking OPN exhibit greater LV chamber dilation after MI with reduced collagen deposition (2). Using adult rat cardiac fibroblasts, we have provided evidence that OPN inhibits interleukin-1β-stimulated increases in MMPs (MMP-2 and −9) expression and activity (17). The major finding of the present study is that MMP inhibition improves cardiac function in mice lacking OPN after MI. Expression and activity of MMPs (MMP-2 and MMP-9) increases in the infarct LV region of both WT and KO mice 3 days post-MI. However, increase in the expression and activity of MMPs in the non-infarct LV was only observed in the myocardium of mice lacking OPN. MMP-9 activity was undetectable using in-gel zymography, MMP-2 activity increased in the non-infarct LV of both groups 14 days post-MI. However, the increase in MMP-2 activity was significantly higher in mice lacking OPN. MMP inhibition decreased MMP-2 activity only in OPN KO group with no effect on TIMP-2 or TIMP-4 protein levels.

An important aspect of early infarct healing is the deposition of collagen, which stabilizes the damaged myocardium (31,32). OPN plays an important role in regulating the synthesis and/or deposition of extracellular matrix (ECM) proteins, including collagen (33). Expression of OPN increases in the heart post-MI (2). OPN modulates the activity of MMP-2 in various cell types (15–17). We have provided evidence that lack of OPN in the heart results in reduced collagen deposition in the heart post-MI (2). Here we show that expression and activity of MMP-2 and MMP-9 is significantly higher in the non-infarct LV in mice lacking OPN 3 days post-MI. The increase in MMP-2 activity in the KO group persisted over the next 14 days. These data suggest that increased OPN expression in the heart post-MI modulates MMP expression and activity, thereby playing an important role in regulation of collagen deposition and fibrosis. It is interesting to note that expression and activity of MMP-2 and MMP-9 increased to a similar extent in the area of infarct in both groups 3 days post-MI. This may relate to the infiltration of neutrophils and macrophages expressing MMPs in the area of infarct (29).

Using Langendorff-perfusion analysis, our laboratory provided evidence that lack of OPN results in greater LV dilation in mice lacking OPN with reduced collagen deposition in the heart 30 days post-MI (2). In this study, using echocardiography and Langendorff perfusion analyses we confirm our previous findings and provide evidence of greater systolic dysfunction in mice lacking OPN 14 days post-MI. MI decreased %FS and EF (%) to a greater extent in mice lacking OPN when compared to WT. Interestingly, MMP inhibition improved heart function in both WT and KO mice. However, the improvement in heart function was significantly higher in mice lacking OPN. MMP-2 and MMP-9, expressed in the heart by cardiac myocytes and fibroblasts, are implicated in the progression of left ventricular dilation and development of heart failure. Activation of MMP, specifically MMP-2, is suggested to decrease cardiac tissue tensile strength and cause systolic and diastolic dysfunction (34,35). Cardiac specific expression of MMP-2 induces development of cardiac contractile dysfunction in the absence of superimposed injury (36). Targeted deletion of MMP-2 attenuates early rupture and improves %FS in mice post MI (13). Similar changes were observed in transgenic mice expressing active MMP-2 driven by the alpha-myosin heavy chain promoter (12). We observed increased MMP-2, not MMP-9, activity in the non-infarct LV only in mice lacking OPN 14 days post-MI. This increase in MMP-2 activity was inhibited by MMP inhibition. Collectively, these studies suggest that interplay of OPN and MMP-2 may play an important role in the regulation of heart function post-MI.

LV chamber enlargement post-MI occurs due to infarct expansion and dilatation of the non-infarcted myocardium. Infarct size measured morphometrically as a fraction of total LV circumference was same in WT and KO hearts post-MI with or without MMP inhibition, suggesting that change in chamber enlargement is most likely due to dilatation of non-infarcted myocardium. Dilatation of the non-infarct LV can occur due to a number of mechanisms including cardiac myocyte apoptosis (37) and/or side-to-side slippage of the myocytes (38) in the absence of increased fibrosis. TUNEL-staining assay indicated no significant increase in the number of apoptotic myocytes post-MI in either group. MMP inhibition had no effect on the number of apoptotic cardiac myocytes. Quantitative analysis of fibrosis using trichrome-stained sections indicated that MI increases fibrosis in both groups. However, the increase in fibrosis was significantly lower in mice lacking OPN. These findings are consistent with our previous observations in the heart 30 days post-MI. The new finding of this study is that MMP inhibition increased fibrosis while decreasing chamber diameter in the myocardium of mice lacking OPN. Together, these data suggests OPN affects collagen deposition (fibrosis) by modulating MMP activity, thereby playing an important role in post-MI LV remodeling.

Previously, OPN is shown to participate in the hypertrophic response of cardiac myocytes in response to pressure overload (3). HW/BW ratio and Myocyte cross-sectional area was higher in WT-MI vs KO-MI. Inhibition of MMP increased HW/BW ratio and myocyte cross-sectional area only in mice lacking OPN. These data suggest that OPN-mediated regulation of MMPs may play an important role in cardiac myocyte hypertrophy. Dynamics of ECM and its interaction with cardiac myocytes during mechanical stretch are implicated in the hypertrophy process (39). Since the components of ECM are substrates for the MMPs, the proteolytic property of MMPs might trigger intracellular signaling cascade involved in mechanical stretch-induced hypertrophy (40–42). However, the precise role of OPN and MMPs in the development of myocyte hypertrophy requires further investigation. Of note, lack of MMP-2 is shown to be associated with reduced cardiac myocyte hypertrophy in response to pressure overload (43).

MMPs degrade various components of the ECM, therefore, MMP activity is tightly regulated in order to check excessive matrix degradation. TIMPs (TIMP-1, −2, −3 and −4), a group of endogenous proteins, inhibit MMP activity (6,8,30,44). TIMPs bind to the active site of the MMPs in a stoichiometric 1:1 molar ratio, thereby blocking access to extracellular matrix substrates. TIMP-4 shows a high level of expression in human myocardial tissue, while the

concentration of TIMP-2 is suggested to determine the role of TIMP-2 in the activation of MMP-2. At low concentrations, TIMP-2 may serve as a receptor for pro-MMP-2, whereas at higher concentrations, TIMP-2 may neutralize MT1-MMP and prevent MMP-2 activation (45). Western blot analyses of LV lysates indicated no change in TIMP-2 and TIMP-4 protein levels in the non-infarct LV between WT or KO group 14 days post-MI. MMP inhibition had no effect on TIMP-2 or TIMP-4 protein levels in WT or KO groups, suggesting MMP inhibition does not affect expression of TIMP-2 and TIMP-4 in the presence or absence of OPN.

Conclusion

The data presented here provide first direct evidence that deficiency of OPN may increase MMP-2 activity leading to reduced compensatory hypertrophy and decreased interstitial fibrosis. These changes might contribute to LV chamber dilatation resulting in cardiac dysfunction. Our findings provide evidence that MMP-mediated adverse myocardial remodeling in response to MI is attenuated by the presence of OPN in the heart.

Perspectives

Although compensatory responses such as hypertrophy and fibrosis may initially preserve LV function, continued maladaptive structural remodeling may lead to the development of heart failure. Defining the processes that can shift the balance from compensatory hypertrophy and fibrosis to decompensated heart failure may have important clinical implications. The present study demonstrated that lack of OPN results in increased MMPs expression and activity which is associated with decreased fibrosis, hypertrophy and cardiac function. Increased cardiac fibrosis and hypertrophy leading to improved cardiac function achieved by MMP inhibition may have use in preventing the development of maladaptive myocardial remodeling post-MI during deficiency of OPN.

Acknowledgements

This work is supported by National Institutes of Health grants HL-071519 (KS) and HL-091405 (KS), a Merit Review Grant from the Department of Veterans Affairs (KS), and a postdoctoral fellowship from the American Heart Association, Southeast Affiliate No. 0525338B (PK).

References

1. Denhardt DT, Noda M, O'Regan AW, Pavlin D, Berman JS. Osteopontin as a means to cope with environmental insults: regulation of inflammation, tissue remodeling, and cell survival. J Clin Invest 2001;107:1055–1061. [PubMed: 11342566]
2. Trueblood NA, Xie Z, Communal C, Sam F, Ngoy S, Liaw L, Jenkins AW, Wang J, Sawyer DB, Bing OH, Apstein CS, Colucci WS, Singh K. Exaggerated left ventricular dilation and reduced collagen deposition after myocardial infarction in mice lacking osteopontin. Circ Res 2001;88:1080–1087. [PubMed: 11375279]
3. Xie Z, Singh M, Singh K. Osteopontin modulates myocardial hypertrophy in response to chronic pressure overload in mice. Hypertension 2004;44:826–831. [PubMed: 15534078]
4. Ashizawa N, Graf K, Do YS, Nunohiro T, Giachelli CM, Meehan WP, Tuan TL, Hsueh WA. Osteopontin is produced by rat cardiac fibroblasts and mediates A(II)-induced DNA synthesis and collagen gel contraction. J Clin Invest 1996;98:2218–2227. [PubMed: 8941637]
5. Singh K, Sirokman G, Communal C, Robinson KG, Conrad CH, Brooks WW, Bing OH, Colucci WS. Myocardial osteopontin expression coincides with the development of heart failure. Hypertension 1999;33:663–670. [PubMed: 10024324]
6. Ahmed SH, Clark LL, Pennington WR, Webb CS, Bonnema DD, Leonardi AH, McClure CD, Spinale FG, Zile MR. Matrix metalloproteinases/tissue inhibitors of metalloproteinases: relationship between changes in proteolytic determinants of matrix composition and structural, functional, and clinical manifestations of hypertensive heart disease. Circulation 2006;113:2089–2096. [PubMed: 16636176]

7. Chapman RE, Spinale FG. Extracellular protease activation and unraveling of the myocardial interstitium: critical steps toward clinical applications. Am.J.Physiol Heart Circ.Physiol 2004;286:H1–H10. [PubMed: 14684355]
8. Mori S, Gibson G, McTiernan CF. Differential expression of MMPs and TIMPs in moderate and severe heart failure in a transgenic model. J Card Fail 2006;12:314–325. [PubMed: 16679266]
9. Spinale FG. Matrix metalloproteinases: regulation and dysregulation in the failing heart. Circ Res 2002;90:520–530. [PubMed: 11909815]
10. Aimes RT, Quigley JP. Matrix metalloproteinase-2 is an interstitial collagenase. Inhibitor-free enzyme catalyzes the cleavage of collagen fibrils and soluble native type I collagen generating the specific 3/4-and 1/4-length fragments. J Biol Chem 1995;270:5872–5876. [PubMed: 7890717]
11. Visse R, Nagase H. Matrix metalloproteinases and tissue inhibitors of metalloproteinases: structure, function, and biochemistry. Circ Res 2003;92:827–839. [PubMed: 12730128]
12. Bergman MR, Teerlink JR, Mahimkar R, Li L, Zhu BQ, Nguyen A, Dahi S, Karliner JS, Lovett DH. Cardiac matrix metalloproteinase-2 expression independently induces marked ventricular remodeling and systolic dysfunction. Am J Physiol Heart Circ Physiol 2007;292:H1847–H1860. [PubMed: 17158653]
13. Hayashidani S, Tsutsui H, Ikeuchi M, Shiomi T, Matsusaka H, Kubota T, Imanaka-Yoshida K, Itoh T, Takeshita A. Targeted deletion of MMP-2 attenuates early LV rupture and late remodeling after experimental myocardial infarction. Am J Physiol Heart Circ Physiol 2003;285:H1229–H1235. [PubMed: 12775562]
14. Menon B, Singh M, Singh K. Matrix metalloproteinases mediate beta-adrenergic receptor-stimulated apoptosis in adult rat ventricular myocytes. Am J Physiol Cell Physiol 2005;289:C168–C176. [PubMed: 15728709]
15. Nemir M, Bhattacharyya D, Li X, Singh K, Mukherjee AB, Mukherjee BB. Targeted inhibition of osteopontin expression in the mammary gland causes abnormal morphogenesis and lactation deficiency. J Biol Chem 2000;275:969–976. [PubMed: 10625634]
16. Philip S, Bulbule A, Kundu GC. Osteopontin stimulates tumor growth and activation of promatrix metalloproteinase-2 through nuclear factor-kappa B-mediated induction of membrane type 1 matrix metalloproteinase in murine melanoma cells. J Biol Chem 2001;276:44926–44935. [PubMed: 11564733]
17. Xie Z, Singh M, Siwik DA, Joyner WL, Singh K. Osteopontin inhibits interleukin-1beta-stimulated increases in matrix metalloproteinase activity in adult rat cardiac fibroblasts: role of protein kinase C-zeta. J Biol Chem 2003;278:48546–48552. [PubMed: 14500723]
18. Giachelli CM, Liaw L, Murry CE, Schwartz SM, Almeida M. Osteopontin expression in cardiovascular diseases. Ann NY Acad Sci 1995;760:109–126. [PubMed: 7785890]
19. Singh M, Ananthula S, Milhorn DM, Krishnaswamy G, Singh K. Osteopontin: A novel inflammatory mediator of cardiovascular disease. Front Biosci 2007;12:214–221. [PubMed: 17127294]
20. Weber GF, Ashkar S, Glimcher MJ, Cantor H. Receptor-ligand interaction between CD44 and osteopontin (Eta-1). Science 1996;271:509–512. [PubMed: 8560266]
21. Liaw L, Birk DE, Ballas CB, Whitsitt JS, Davidson JM, Hogan BL. Altered wound healing in mice lacking a functional osteopontin gene (spp1). J Clin Invest 1998;101:1468–1478. [PubMed: 9525990]
22. Krishnamurthy P, Subramanian V, Singh M, Singh K. Deficiency of beta1 integrins results in increased myocardial dysfunction after myocardial infarction. Heart 2006;92:1309–1315. [PubMed: 16547211]
23. Peterson JT, Hallak H, Johnson L, Li H, O'Brien PM, Sliskovic DR, Bocan TM, Coker ML, Etoh T, Spinale FG. Matrix metalloproteinase inhibition attenuates left ventricular remodeling and dysfunction in a rat model of progressive heart failure. Circulation 2001;103:2303–2309. [PubMed: 11342481]
24. Ikonomidis JS, Hendrick JW, Parkhurst AM, Herron AR, Escobar PG, Dowdy KB, Stroud RE, Hapke E, Zile MR, Spinale FG. Accelerated LV remodeling after myocardial infarction in TIMP-1-deficient mice: effects of exogenous MMP inhibition. Am J Physiol Heart Circ Physiol 2005;288:H149–H158. [PubMed: 15598866]

25. Hoit BD, Khoury SF, Kranias EG, Ball N, Walsh RA. In vivo echocardiographic detection of enhanced left ventricular function in gene-targeted mice with phospholamban deficiency. Circ Res 1995;77:632–637. [PubMed: 7641333]
26. Kudej RK, Iwase M, Uechi M, Vatner DE, Oka N, Ishikawa Y, Shannon RP, Bishop SP, Vatner SF. Effects of chronic beta-adrenergic receptor stimulation in mice. J Mol Cell Cardiol 1997;29:2735–2746. [PubMed: 9344768]
27. Krishnamurthy P, Subramanian V, Singh M, Singh K. {beta}1 Integrins Modulate {beta}-Adrenergic Receptor-Stimulated Cardiac Myocyte Apoptosis and Myocardial Remodeling. Hypertension 2007;49:865–872. [PubMed: 17283249]
28. Mukherjee R, Mingoia JT, Bruce JA, Austin JS, Stroud RE, Escobar GP, McClister DM Jr, Allen CM, Alfonso-Jaume MA, Fini ME, Lovett DH, Spinale FG. Selective spatiotemporal induction of matrix metalloproteinase-2 and matrix metalloproteinase-9 transcription after myocardial infarction. Am J Physiol Heart Circ Physiol 291:H2216–H2228. [PubMed: 16766634]
29. Tao ZY, Cavasin MA, Yang F, Liu YH, Yang XP. Temporal changes in matrix metalloproteinase expression and inflammatory response associated with cardiac rupture after myocardial infarction in mice. Life Sci 2004;74:1561–1572. [PubMed: 14729404]
30. Vanhoutte D, Schellings M, Pinto Y, Heymans S. Relevance of matrix metalloproteinases and their inhibitors after myocardial infarction: a temporal and spatial window. Cardiovasc Res 2006;69:604–613. [PubMed: 16360129]
31. Ertl G, Frantz S. Wound model of myocardial infarction. Am J Physiol Heart Circ Physiol 2005;288:H981–H983. [PubMed: 15706047]
32. Jugdutt BI, Joljart MJ, Khan MI. Rate of collagen deposition during healing and ventricular remodeling after myocardial infarction in rat and dog models. Circulation 1996;94:94–101. [PubMed: 8964124]
33. Satoh M, Nakamura M, Akatsu T, Shimoda Y, Segawa I, Hiramori K. Myocardial osteopontin expression is associated with collagen fibrillogenesis in human dilated cardiomyopathy. Eur J Heart Fail 2005;7:755–762. [PubMed: 16087132]
34. Mujumdar VS, Smiley LM, Tyagi SC. Activation of matrix metalloproteinase dilates and decreases cardiac tensile strength. Int J Cardiol 2001;79:277–286. [PubMed: 11461752]
35. Mujumdar VS, Tyagi SC. Temporal regulation of extracellular matrix components in transition from compensatory hypertrophy to decompensatory heart failure. J Hypertens 1999;17:261–270. [PubMed: 10067796]
36. Wang GY, Bergman MR, Nguyen AP, Turcato S, Swigart PM, Rodrigo MC, Simpson PC, Karliner JS, Lovett DH, Baker AJ. Cardiac transgenic matrix metalloproteinase-2 expression directly induces impaired contractility. Cardiovasc Res 2006;69:688–696. [PubMed: 16183043]
37. Hayakawa Y, Chandra M, Miao W, Shirani J, Brown JH, Dorn GW, Armstrong RC, Kitsis RN. Inhibition of cardiac myocyte apoptosis improves cardiac function and abolishes mortality in the peripartum cardiomyopathy of Galpha(q) transgenic mice. Circulation 2003;108:3036–3041. [PubMed: 14638549]
38. Olivetti G, Capasso JM, Sonnenblick EH, Anversa P. Side-to-side slippage of myocytes participates in ventricular wall remodeling acutely after myocardial infarction in rats. Circ Res 1990;67:23–34. [PubMed: 2364493]
39. Yutao X, Geru W, Xiaojun B, Tao G, Aiqun M. Mechanical stretch-induced hypertrophy of neonatal rat ventricular myocytes is mediated by beta(1)-integrin-microtubule signaling pathways. Eur J Heart Fail 2006;8:16–22. [PubMed: 16198630]
40. Milkiewicz M, Mohammadzadeh F, Ispanovic E, Gee E, Haas TL. Static strain stimulates expression of matrix metalloproteinase-2 and VEGF in microvascular endothelium via JNK-and ERK-dependent pathways. J Cell Biochem 2007;100:750–761. [PubMed: 17031856]
41. Wang TL, Yang YH, Chang H, Hung CR. Angiotensin II signals mechanical stretch-induced cardiac matrix metalloproteinase expression via JAK-STAT pathway. J Mol Cell Cardiol 2004;37:785–794. [PubMed: 15350851]
42. Zhou C, Ziegler C, Birder LA, Stewart AF, Levitan ES. Angiotensin II and stretch activate NADPH oxidase to destabilize cardiac Kv4.3 channel mRNA. Circ Res 2006;98:1040–1047. [PubMed: 16556864]

43. Matsusaka H, Ide T, Matsushima S, Ikeuchi M, Kubota T, Sunagawa K, Kinugawa S, Tsutsui H. Targeted deletion of matrix metalloproteinase 2 ameliorates myocardial remodeling in mice with chronic pressure overload. Hypertension 2006;47:711–717. [PubMed: 16505197]

44. Spinale FG. Myocardial matrix remodeling and the matrix metalloproteinases: Influence on cardiac form and function. Physiol Rev 2007;87:1285–1342. [PubMed: 17928585]

45. Li YY, McTiernan CF, Feldman AM. Interplay of matrix metalloproteinases, tissue inhibitors of metalloproteinases and their regulators in cardiac matrix remodeling. Cardiovasc Res 2000;46:214–224. [PubMed: 10773225]

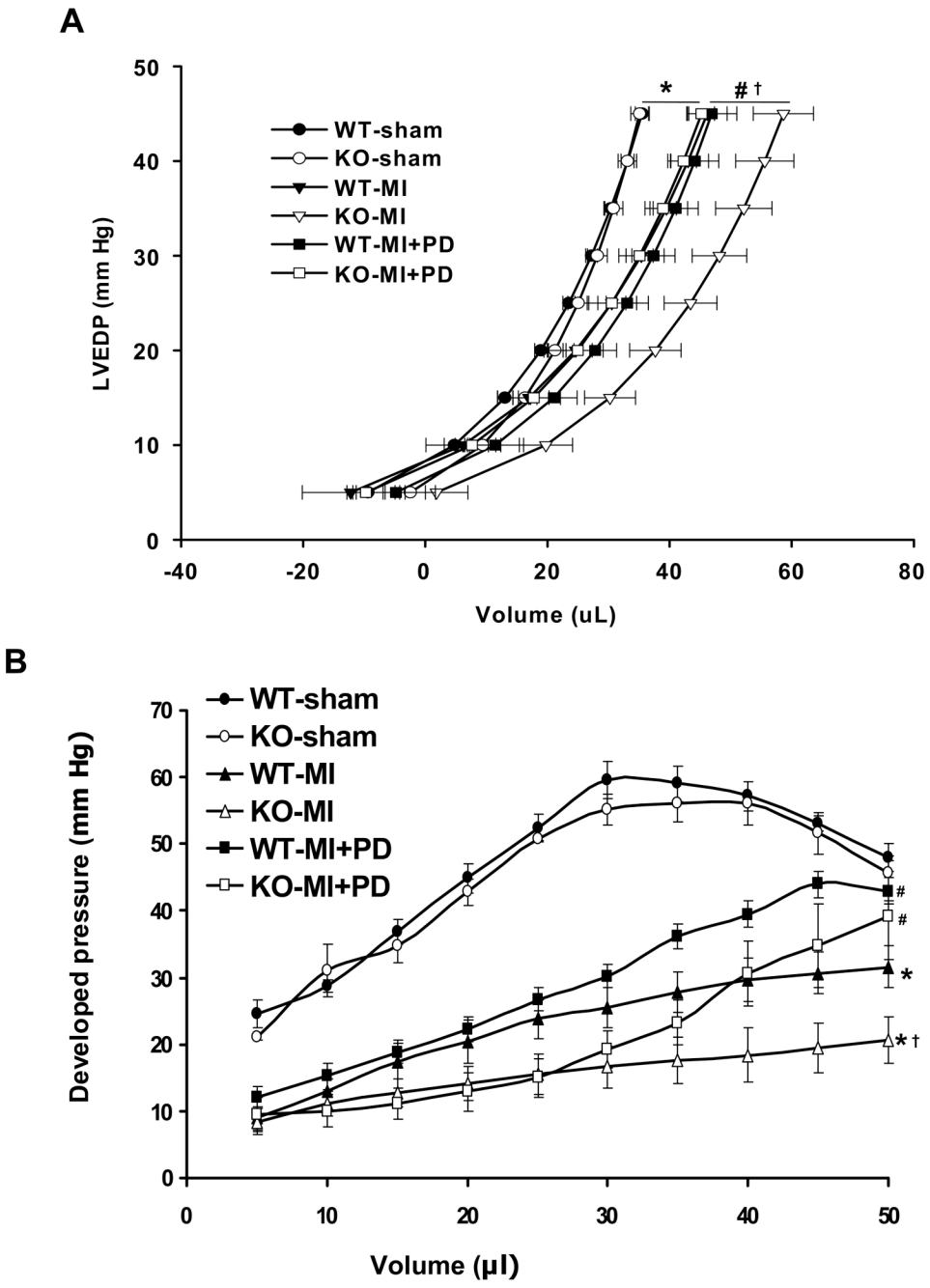

Figure 1.

A. Analysis of LV end-diastolic pressure-volume relationships 14 days post-MI. KO-MI group exhibited a rightward shift when compared to WT-MI and sham. *P<0.05 vs. sham; †P<0.05 vs. WT-MI; #P<0.05 vs. KO-MI+PD; n=6 except sham groups (n=5). **B**. Analysis of LV developed pressure versus volume 14 days post-MI. KO-MI group showed significant decrease in the LV developed pressure for a given volume. MMP inhibition increased LVDP at >35 µl volume. *P<0.05 vs. sham; †P<0.05 vs. WT-MI; #P<0.05 vs. KO-MI or WT-MI; n=6 except sham groups (n=5).

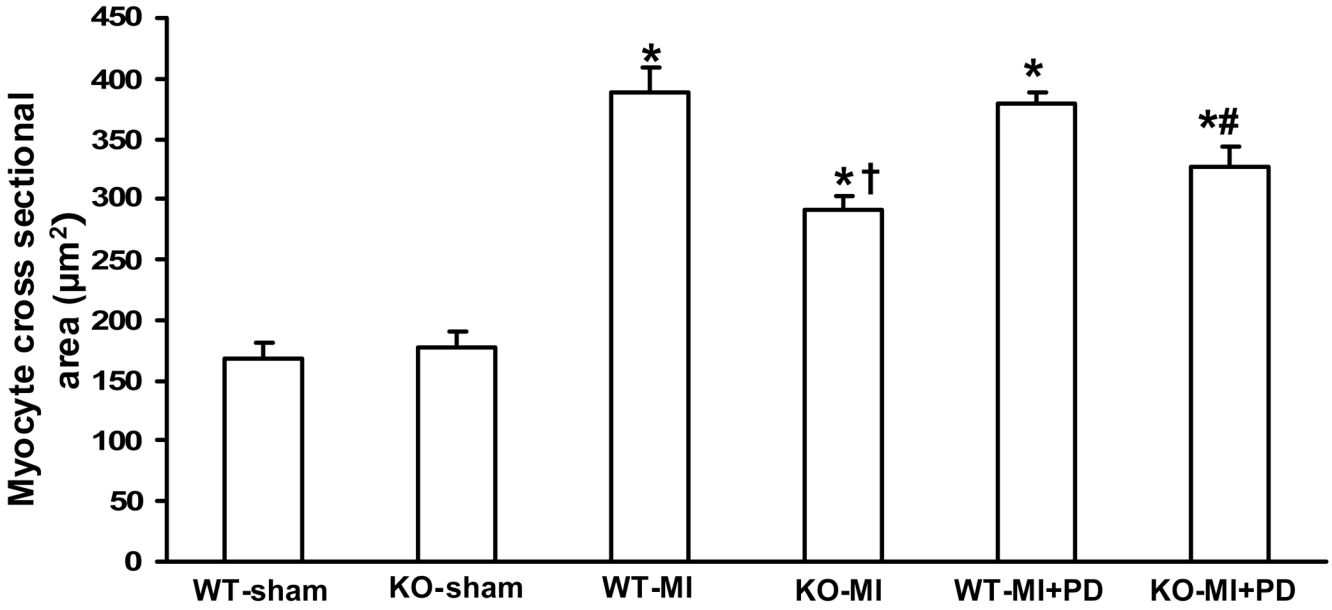

Figure 2.

Quantitative analysis of myocyte cross-sectional area 14 days post-MI. WT-MI showed increased myocyte cross-sectional area as compared to KO-MI and sham groups. MMP inhibition increased myocyte cross-sectional area in KO-MI, not in WT-MI. *P<0.001 vs. WT-sham; †P<0.001 vs KO-MI; #P<0.05 vs KO-MI; n=5.

Figure 3A

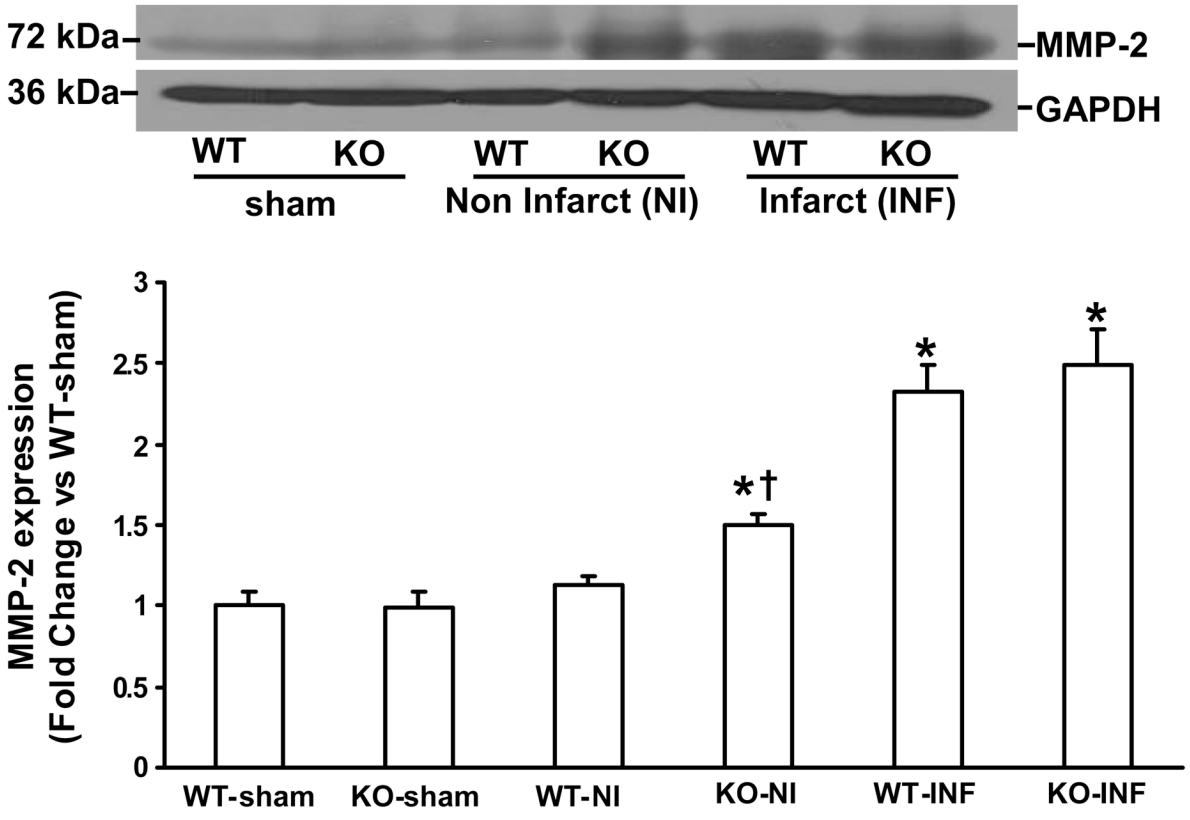

Figure 3B

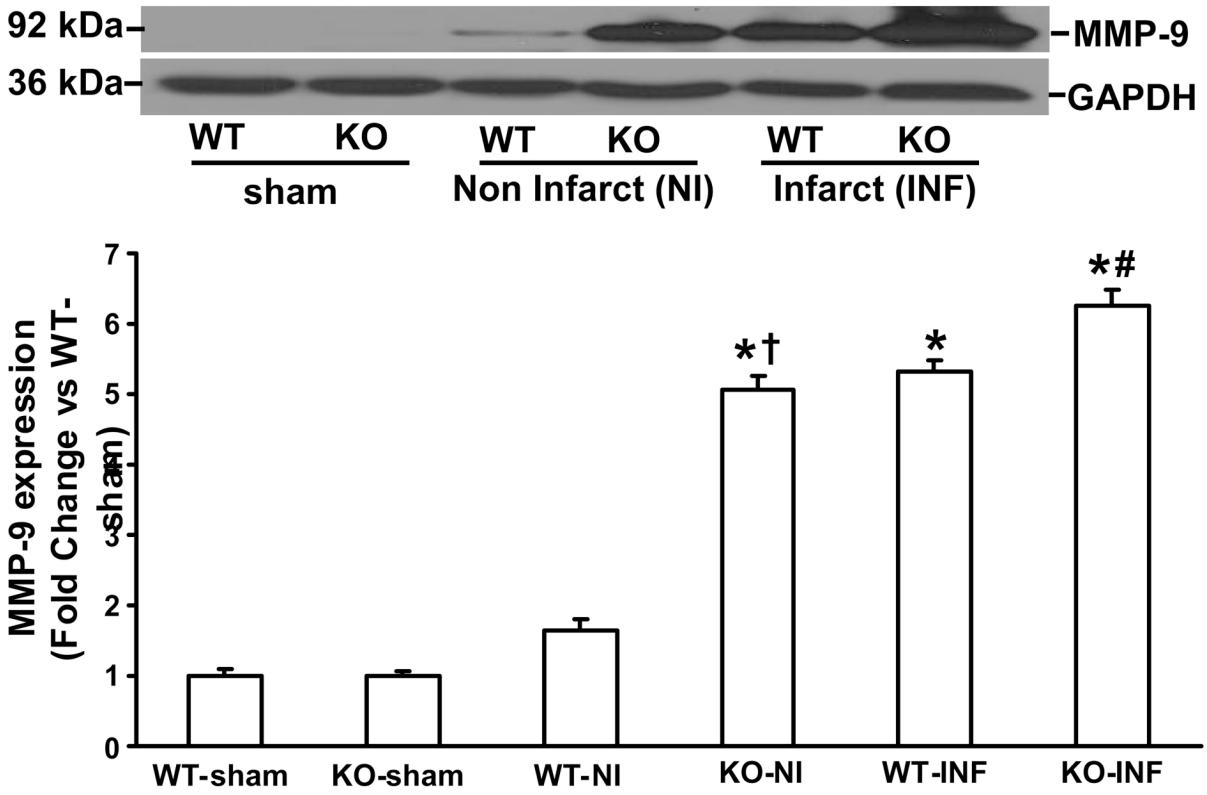

Figure 3.

A. MMP-2 protein expression in the left ventricles 3 days post-MI. Total LV lysates were analyzed by Western blot using anti-MMP-2 antibodies. Equal loading of proteins in each lane is indicated by GAPDH immunostaining. The lower panel exhibits the mean data normalized to GAPDH. MMP-2 was higher in non-infarct area, *P<0.05 vs sham; †P<0.05 vs WT-NI; n=3.

B. MMP-9 protein expression in the left ventricle 3 days post-MI. Total LV lysates were analyzed by Western blot using anti-MMP-9 antibodies. The lower panel exhibits the mean data normalized to GAPDH. MMP-9 was higher in non-infarct area, *P<0.001 KO-INF vs sham; †P<0.05 vs WT-INF; n=3. NI, non-infarct area; INF, infarct area.

Figure 4A

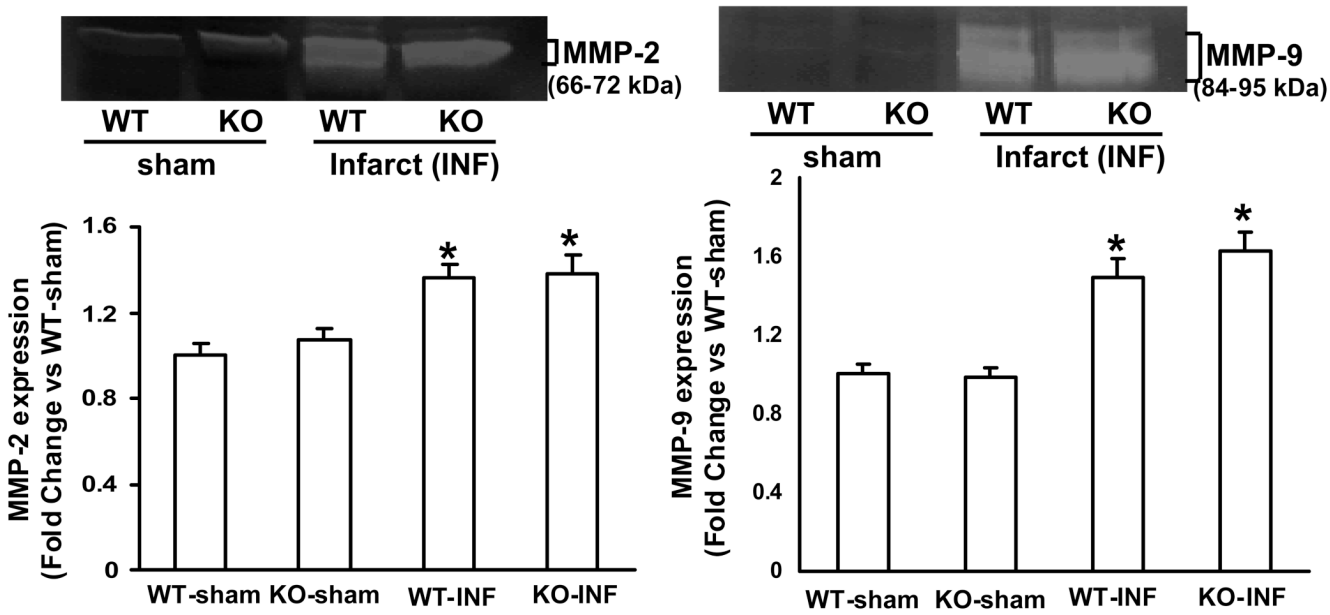

Figure 4B

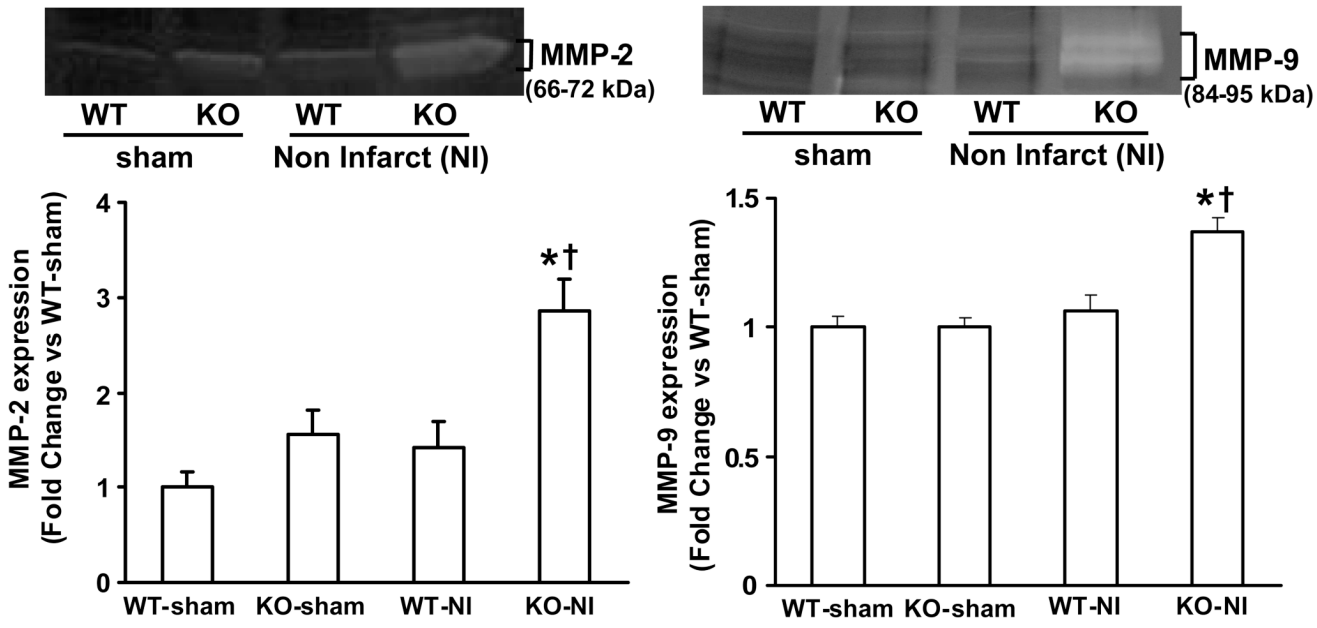

Figure 4.

A. Gelatin in-gel zymography of infarct area of LV tissue 3 days post-MI. The lower panel exhibits the mean densitometry values for MMP-2 (left) and MMP-9 (right). MMP-2 and MMP-9 was higher in MI groups as compared to sham groups, *P<0.05 vs sham; n=3. **B**. Gelatin in-gel zymography of non-infarct area of LV tissue 3 days post-MI. The lower panel exhibits the mean densitometry values for MMP-2 (left) and MMP-9 (right). MMP-2 and MMP-9 was higher in KO-NI group as compared to WT-NI and sham groups. MMP-2, *P<0.05 vs sham, †P<0.05 vs WT-NI; MMP-9, *P<0.01 vs sham, †P<0.05 vs WT-NI; n=3.

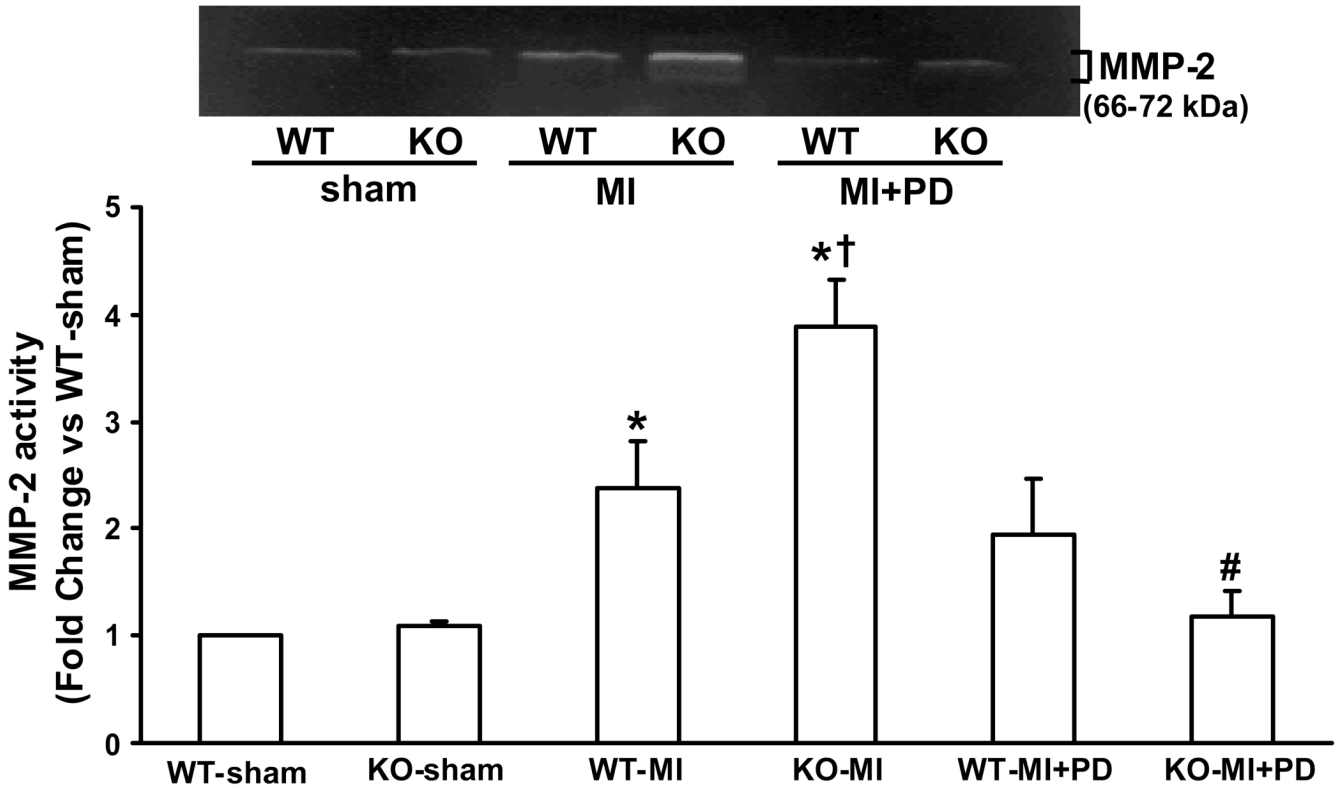

Figure 5.

Gelatin in-gel zymography of non-infarct area of LV tissue 14 days post-MI. The lower panel exhibits the mean densitometry values for MMP-2. MMP-2 activity was higher in KO-MI group as compared to WT-MI and sham groups. MMP inhibition decreased MMP-2 activity in KO-MI. *P<0.01 vs sham, †P<0.05 vs. WT-MI, $^{\#}$P<0.01 vs. KO-MI ; n=4.

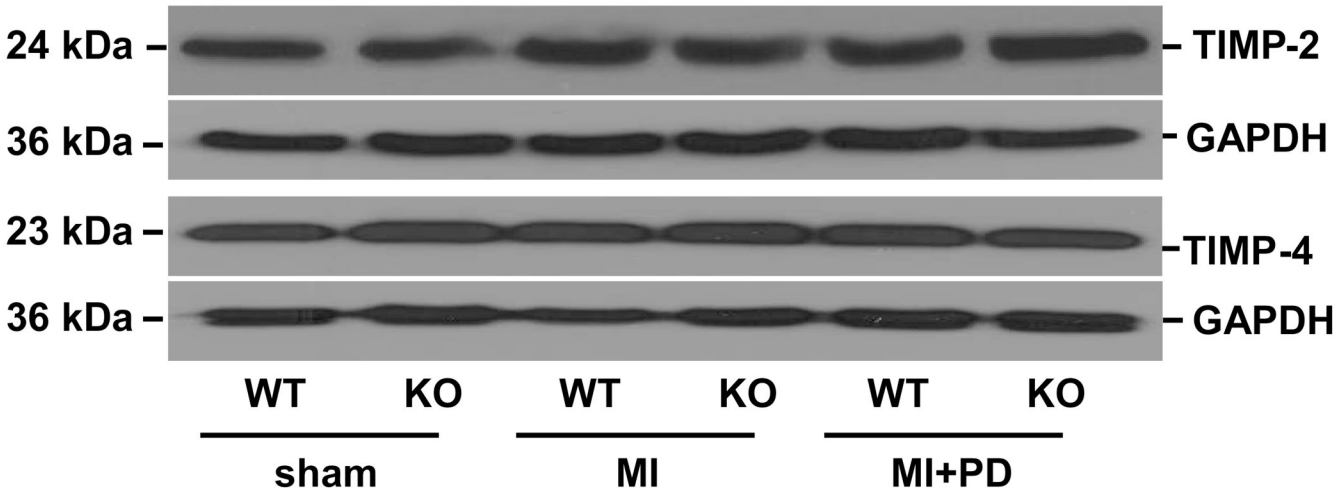

Figure 6.
TIMP-2 and TIMP-4 protein expression in the non-infarct area of LV tissue 14 days post-MI. Total LV lysates were analyzed by Western blot using anti-TIMP-2 and -4 antibodies. Equal loading of proteins in each lane is indicated by GAPDH immunostaining; n=4.

Table 1

Morphometric and LV measurements (14 days post-MI)

Parameters	WT-sham	KO-sham	WT-MI	KO-MI	WT-MI+PD	KO-MI+PD	P value
Body weight, g	29.52±2.52	35.20±2.42	27.90±2.42	31.91±3.73	28.17±3.17	28.74±5.88	-
Infarct size, %LV circumference	-	-	53.02±1.29	50.49±2.31	52.36±2.08	51.35±2.81	-
Heart/Body weight ratio, mg/g	5.51±0.19	5.88±0.28	9.57±0.83*†	7.70±1.11*	9.51±0.43	9.57±1.83$^{\#}$	*<0.01; †<0.05; $^{\#}$<0.05
LV Fibrosis, % pixel	0.18±0.03	0.17±0.01	22.42±3.20*†	9.80±0.99*	20.69±1.14	18.39±2.39$^{\#}$	*<0.001; †<0.005; $^{\#}$<0.01

Values are mean±SE; n=5 in each group

*comparison between sham and MI within genotype

†comparison between MI groups

$^{\#}$comparison between MI+PD and MI within genotype

Table 2

Echocardiographic measurements (14 days post-MI)

Parameters	WT-sham	KO-sham	WT-MI	KO-MI	WT-MI+PD	KO-MI+PD	P value
LVEDD (mm)	4.00±0.07	4.00±0.07	5.45±0.26*	6.03±0.13*†	5.13±0.13 (−6.37)	5.20±0.21 (−15.92)$^{\#}$	*<0.001; †<0.05; $^{\#}$<0.01
LVESD (mm)	2.92±0.08	2.99±0.07	4.56±0.22*	5.21±0.14*†	4.03±0.17 (−12.94)	4.12±0.30 (−26.46)$^{\#}$	*<0.001; †<0.05; $^{\#}$<0.01
LVSWd (mm)	0.46±0.02	0.50±0.02	0.75±0.02*	0.67±0.02*†	0.73±0.02 (−1.58)	0.73±0.03 (+8.48)$^{\#}$	*<0.001; †<0.05; $^{\#}$<0.05
LVSWs (mm)	0.64±0.01	0.65±0.01	0.86±0.01*	0.82±0.05*	0.88±0.02 (+1.51)	0.95±0.01 (+13.37)$^{\#}$	*<0.001; $^{\#}$<0.05
FS (%)	27.19±1.19	28.11±1.20	16.44±0.70*	13.65±1.24*†	21.38±1.76 (+23.11) $^{\#}$	21.19±2.71 (+35.57)$^{\#}$	*<0.001; †<0.05; $^{\#}$<0.05
EF (%)	53.33±1.89	54.52±1.84	34.04±1.28*	28.50±2.35*†	42.89±3.06 (+20.64) $^{\#}$	42.32±4.72 (+32.66)$^{\#}$	*<0.001; †<0.05; $^{\#}$<0.05
Heart rate (bpm)	354±9.30	368±7.99	395±15.16	411±17.40	419±18.75	433±21.89	-

Values are mean±SE; n=5 in each group; LVEDD, LV end-diastolic diameter; LVESD, LV end-systolic diameter; LVDSW, LV septal wall thickness in diastole; LVSSW, LV septal wall thickness in systole; %FS, percent fractional shortening; %EF, percent ejection fraction; bpm, beats per minute

*comparison between sham and MI within genotype

†comparison between MI groups

$^{\#}$comparison between MI+PD and MI within genotype; Figures in parenthesis indicate percent increase or decrease from their respective MI values.

Mol Cell Biochem. Author manuscript; available in PMC 2009 August 1.